Key Engineering Materials Vol. 457 (2011) pp 361-366

doi:10.4028/www.scientific.net/KEM.457.361

Effect of Selected Alloying Elements on Mechanical Properties of Pearlitic Nodular Cast Irons

Joan Serrallach[1,a], Jacques Lacaze[2,b], Jon Sertucha[3,c], Ramón Suárez[3,d], Adrián Monzón[1,e]

[1]INFUN, S. A., Camí Can Ubach 25, 08620 Sant Vicenç dels Horts (Barcelona), Spain

[2]CIRIMAT, Université de Toulouse, ENSIACET, B.P. 44362, 31432 Toulouse cedex 4, France

[3]Engineering and Foundry Department, AZTERLAN, Aliendalde auzunea 6, E-48200 Durango (Bizkaia), Spain

[a]joan.serrallach@infun.es, [b]jacques.lacaze@ensiacet.fr, [c]jon.sertucha@azterlan.es, [d]ramon.suarez@azterlan.es, [e]adrian.monzon@infun.es

Keywords: pearlitic nodular cast-iron, mechanical properties, alloying elements

Abstract. There is a continuous demand for low-cost nodular cast irons with improved mechanical properties, this being an industrial requirement both for pearlitic as well as for ferritic grades. Developments in pearlitic nodular irons should lead to alloys with higher and higher strength while retaining some ductility in the as-cast state so as to respond to demands related to castings for high power automotive engines in competition with steel castings and ADI. According to these aims, several alloying elements have been selected and added separately or combined to standard commercial nodular cast irons. In all cases, only low-level additions were made and their effects on the microstructure and mechanical properties at room temperature have been characterized and are discussed. A statistical analysis has been performed on the data obtained that accounts for changes in alloying additions as well as for variations in process parameters.

Introduction

The ratio of ferrite to pearlite in the matrix of nodular cast irons is known to depend mainly on three parameters: the cooling rate during the eutectoid transformation [1-5], the nodule count resulting from the solidification step [6, 7] and alloying elements [1, 2, 6, 8-13]. An increase of nodule count to decrease the amount of pearlite has been found effective at low nodule counts only [14, 15]. Conversely, avoiding totally the formation of ferrite by increasing the cooling rate is inappropriate for manufacturing usual cast irons under industrial conditions. Hence, promoting a pearlitic structure is most usually achieved by specific additions and the effect of several alloying elements on the microstructure and mechanical properties of nodular cast irons has been studied over many years [1-3, 8, 10-13, 16-21].

Nowadays, there is a strong demand for cheap materials with mechanical properties able to withstand the requirements of high power automotive engines. The current industrial way for achieving the necessary targets is the use of forged steel or austempered nodular iron castings. However the costs linked to these solutions are higher than the ones for manufacturing as-cast nodular iron parts. Thus, there is an opportunity for developing nearly fully pearlitic nodular cast irons, with increased ultimate strength while retaining sufficient elongation, by suitable additions of alloying elements. The aim of the present study was thus to analyse the influence of various alloying elements on the structural features and mechanical properties of pearlitic nodular irons. The effect of selected alloying elements was evaluated together with the possible counter effects of minor elements originating from the use of commercial steel scrap added to the metallic charges.

Experimental Procedures

A total of 85 alloys were prepared in a medium frequency induction furnace (250 Hz, 100 kW) 100 kg in capacity. In all cases, the charge was composed of 30-50% automotive steel scrap and 70-50% low alloyed pig iron, and the composition was adjusted according to the required Mn content which is the main contribution from the steel scrap used. After melting, the carbon, silicon and selected alloying elements contents were checked and adjusted to the specified values. The liquid metal temperature was then increased to 1500-1510ºC and its surface skimmed. Then the melt was treated in a 50 kg capacity ladle with a nodulariser alloy (42-44 wt.% Si, 5-6 wt.% Mg, 0.9-1.0 wt.% Ca, 0.4-0.5 wt.% Al, 0.9-1.1 wt.% RE) by the sandwich method. The treatment temperature was between 1470 and 1490ºC. When the reaction was finished, the Mg-treated batches were transferred to the pouring area. Table 1 lists the range of variation of all the elements measured on the cast parts.

Table 1. Composition range (%, wt) of all elements measured on the cast parts.

	C	Si	Mn	P	S	Mg	Cu	B	Ti	V
Minimum	2.32	1.66	0.12	0.012	0.008	0.026	0.44	0	0	0
Maximum	4.08	2.97	1.06	0.045	0.021	0.060	1.72	0.0067	0.36	0.5
	Sn	Cr	Al	N	Zr	Ni	Mo	Nb	Sb	
Minimum	0	0	0	0	0	0.0045	0	0	0	
Maximum	0.025	0.35	0.02	0.0086	0.005	1.18	0.98	0.46	0.005	

The alloys were then cast in chemically bonded sand moulds that contained standard keel-blocks (Fig. 1-a). The inoculation treatment was carried out by adding approximately 0.15% of a commercial inoculant (68.1 wt.% Si, 0.89 wt.% Al, 1.65 wt.% Ca, 0.45 wt.% Bi, 0.38 wt.% Ba, 0.37 wt.% RE) into the cavity of the moulds. Cooling of the cast keel-blocks was achieved with up to three different conditions: in mould, static air and forced air. For these last two cooling conditions, the keel-blocks were removed from the mould just after solidification was completed and were allowed to cool in air that was either calm or forced. A total of 158 keel-blocks were prepared from the 85 alloys. In a few cases, a cooling curve was recorded by means of a K-type thermocouple positioned just above the area used for mechanical test sampling (Fig. 1-a). Fig. 1-b compares the cooling curves recorded during one of the trials on the keel-blocks cooled in the mould and in static air. From the few curves recorded, the cooling rate of the metal V_r between 1050 and 715°C could be estimated as 15ºC/min for mould cooling, 45ºC/min for air cooling and 90ºC/min for forced cooling. For statistical analysis, it will be assumed that the cooling rate was the same for all the experiments carried out with the same conditions, but limited available information showed in fact large changes from one casting to another.

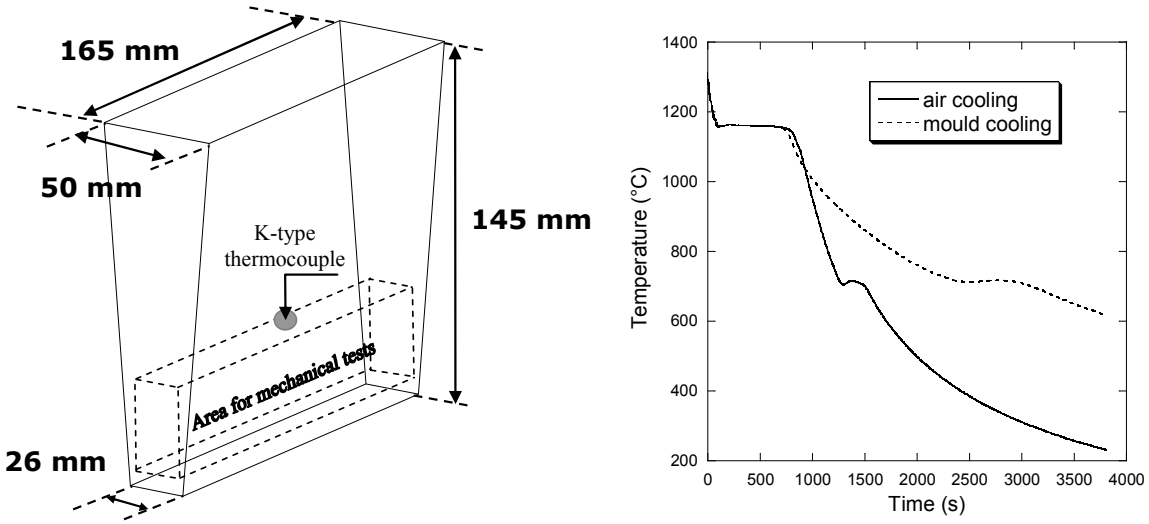

Fig. 1. Keel-block used for all castings (a-left) and example of cooling curves recorded during mould and air cooling (b-right).

After solidification and cooling, one standard tensile strength specimen (10 mm in diameter) was machined from the lower part of each keel-block (see Fig. 1-a) on which the rupture stress UTS, the rupture strain A and the elasticity limit LE were measured. On one of the samples, that had a fully bainitic structure, the LE and A values could not be estimated and the UTS value appeared to be an outlier compared to the rest of the data. This sample was not considered further in the analysis. After the mechanical test, the specimen was used for determination of the Brinell hardness D using a 10 mm diameter sphere and a load of 3000 kg. Finally, the sample was cut and prepared for subsequent metallographic characterisation. The nodule count N_A and the nodularity were evaluated by quantitative image analysis, while the fractions of ferrite f^{α} and pearlite f^{per} were determined by comparing the microstructure obtained after etching with 5% Nital with standard reference microstructures [22, 23]. In a few cases, the matrix was found to contain bainite and in two cases iron carbides were observed. For these latter cases, the fraction of constituents other than ferrite and pearlite was summed as a variable f^{other}.

Statistical Analysis

The statistical analysis was performed using JMP® software. As a first step, a linear multivariate analysis was performed using f^{per} or one of the mechanical parameters as the output variable and all the elements listed in Table 1 as input variables. Looking at the residues, it was found that $(V_r)^{0.5}$ should be considered as a variable rather than V_r. This analysis gave what is expected to be the highest R^2 correlation coefficient because all possible input variables were taken into account. Then, a stepwise analysis was performed during which the software selected successively the most pertinent variables. From this analysis, a model expressing each of the output variables as a first order polynomial of the composition was obtained, that was limited to those input variables that were found relevant at a risk of less than 5%.

Results

Fig. 2 shows the pearlite fraction f^{per} versus nodule count N_A. There are a few points at very low pearlite fraction that do not appear in this graph, which are related to castings having a nearly fully bainitic as-cast matrix due to alloying with Mo and/or Nb. It is seen that no clear correlation shows up from the graph in Fig. 2. As a matter of fact, no simple correlation could be obtained between any of the mechanical properties and microstructure data, either N_A or f^{per}. With the exception of the relation between UTS and A that was highly scattered, relations between mechanical properties showed significant correlation. The best appeared to be between D and A; as illustrated in Fig. 3, it is similar to relations reported before [1].

The fact that the mechanical properties are not well correlated with the pearlite fraction shows that alloying additions affect them strongly. This led to the use of multivariate linear analysis with the whole composition, $(V_r)^{0.5}$ and microstructure parameters (N_A, f^{α}, f^{other}) as input variables. The R^2 coefficients that were obtained are listed in the first column of Table 2. Except in the case of the rupture elongation A, it was observed that the cooling rate V_r is by far the most significant parameter amongst all the variables. The part of the variance due to $(V_r)^{0.5}$ is listed in the second column of Table 2 and explains ≈0.46/0.75, i.e. about 60% of the whole variance of the data set of LE, UTS or D. It was also noted that the R^2 coefficient for A is not as high as for the other mechanical properties; this relates to the higher intrinsic experimental scatter of this parameter as already apparent in the literature [24].

A stepwise analysis was then performed that retained finally a set of input variables found relevant for each of the four mechanical variables. The values of the R^2 coefficients at the end of the stepwise procedure are listed in the last column of Table 2. It is seen that they are quite close to the values in the first column, meaning that the variance is quite properly explained with the selected variables. Due to the importance of the cooling rate, it may be guessed that part of the unexplained variance could be due to a scatter in the V_r values.

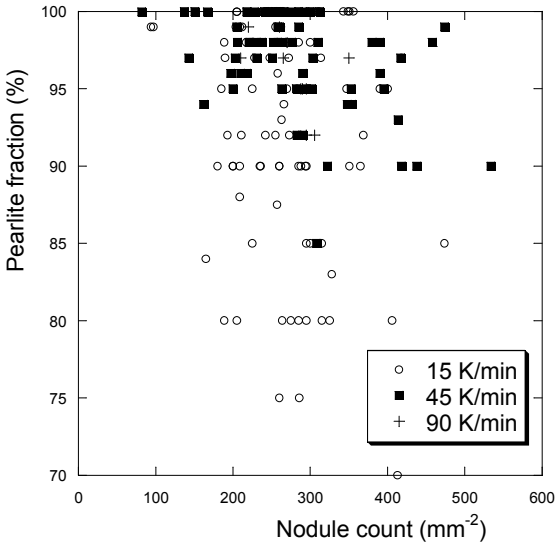

Fig. 2. Pearlite fraction versus nodule count.

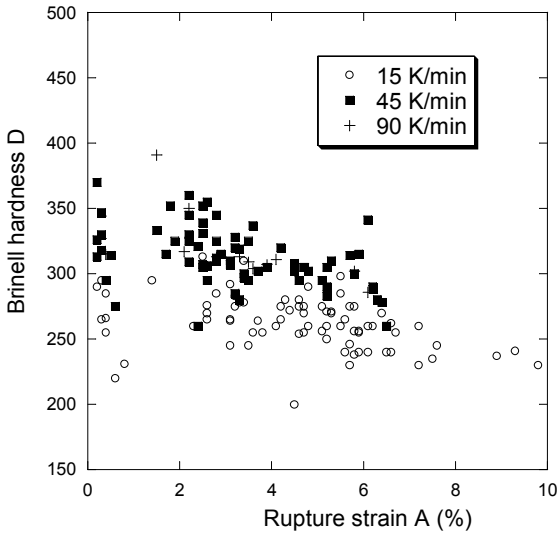

Fig. 3. Hardness versus rupture strain A.

Table 2. R^2 coefficient measured after multivariable analysis with all input variables (composition and microstructure variables) and after step by step analysis by retaining only the variables that appear significant.

Variable	Whole set of variables	Part due to $(V_r)^{0.5}$	Step by step analysis
LE	0.79	0.49	0.77
UTS	0.74	0.45	0.72
A	0.67	0.02	0.64
D	0.78	0.43	0.73

The coefficients obtained at the end of the multivariate analysis are listed in Table 3. They define the model allowing for prediction of each of the mechanical properties as a linear polynomial of the cooling rate $(V_r)^{0.5}$, the composition variables (w_i) found significant and microstructure data (N_A, f^{α}, f^{other}), according to the following equation:

$$\text{Predicted value} = a_0 + a_{Vr} \cdot (V_r)^{0.5} + a_{NA} . N_A + a^{\alpha} \cdot f^{\alpha} + a_{other} \cdot f^{other} + \Sigma a_i \cdot w_i \qquad (1)$$

It is seen in Table 3 that very few composition variables were found statistically significant, and that they may differ from one mechanical property to another. Fig. 4 compares the predicted mechanical properties to the corresponding measured data. Systematic analysis of the residuals showed no trends for the selected input variables, thus confirming the linear model.

Table 2. Regression coefficients obtained by following a stepwise procedure (V_r in $K.min^{-1}$, N_A in mm^{-2}, f^{α} and f^{other} in %, w_i in wt.%, LE and UTS in MPa, A in % and D in HBW).

	constant	$(V_r)^{0.5}$	N_A	f^{α}	f^{other}	C	Cu	Cr	Mg
LE	357.9	32.6		-2.79		-57.3	116.8		2125
UTS	786.8	28.7		-4.92			76.67		
A	1.391	-0.24	0.0052	0.090		1.53		-3.98	-38
D	199.0	11.41	-0.082	-1.57	0.285		21.7		761.7
	Mn	Mo	N	Nb	Ni	P	Sb	Ti	V
LE	104.5	124.5							264.9
UTS		83.5	-8126		-64.0	-3567	-8837	-223.6	154.1
A	-2.26	-1.67		-7.19			-243		-10.0
D		47.7							68.0

Discussion

Most of the previous work mentioned in the introduction looked for the effect of alloying additions on mechanical properties together with change in the microstructure of the material. A few reports dealing with the cooling rate effect have been reviewed by Goodrich and Lobenhofer [4] in a study mainly devoted to the effect of the casting skin as exemplified in small section castings. The present results show that this is the most important variable, explaining about 50% of the variance on hardness, yield and ultimate tensile strength, so that much care should be taken when relating it only to pearlite fraction. Indeed, as this latter parameter was here evaluated separately, the present study shows that the cooling rate affects significantly the mechanical properties of pearlite, e.g. through the fineness of its interlamellar spacing. The fact that clear linear relationships with alloying contents were found is in line with the work by Venugopalan and Alagarsamy [18]. This shows that the non linear relations most often reported in the literature and associated with optimum values of alloying elements [16] relate to microstructure changes that have been here taken into account separately. Such microstructure changes may be the appearance of ferrite, carbides or bainite, or else of degenerate graphite (that was not observed in the present work).

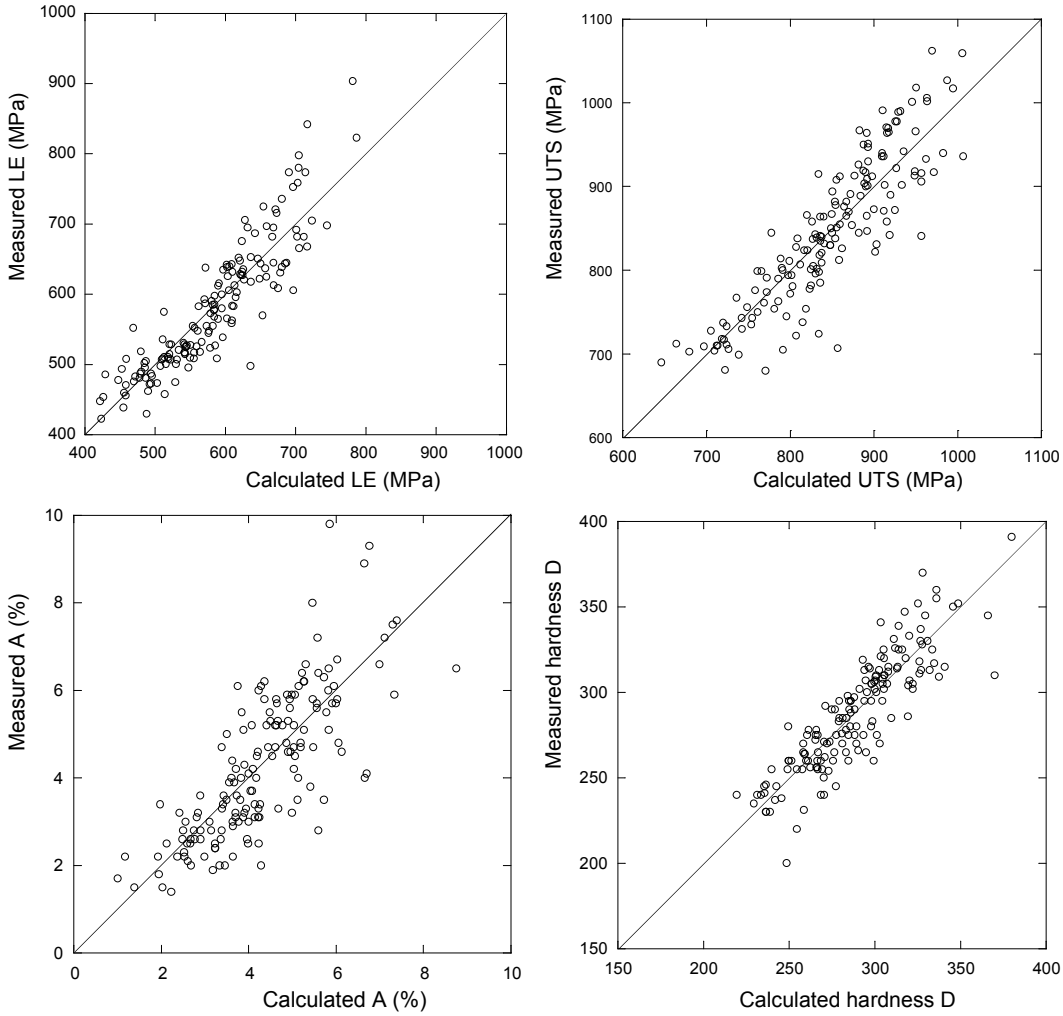

Fig. 4. Comparison of calculated and measured values of LE, UTS, A and D.

Elements such as Cu, Mn, Sn, Sb and Cr are known to increase the volume fraction of pearlite and as such increase tensile strength, yield strength and hardness and decrease elongation and impact energy. It is worth noting that Sn and Cr do not appear in Table 3, meaning that their role should be limited to increasing the pearlite fraction but not to affecting its properties. It is also seen that Sb as well as N decrease UTS; this may be due to precipitation of minor phases that were not detected. Small additions of Mo and Ni were reported to promote the formation of ferrite and

increase ductility [10, 18], but other studies showed that these elements may promote pearlite when the content of the residual elements is low [11, 13, 25]. In the present study, Ni appears detrimental and Mo beneficial to pearlite properties. Additions of Si [21, 26] have shown to increase the volume fraction of ferrite, but this effect seems to be linked to the higher nodule counts obtained when increasing the amount of this element. This is indirectly confirmed in that neither Bi nor Si appear in Table 3, i.e. they may affect the microstructure but not the pearlite mechanical properties. The positive effect of Mg on LE and D and its negative effect on A are certainly worthy of further work.

Conclusion

The statistical analysis performed in this work allows mechanical properties of a specific alloy to be predicted as a function of the square root of the cooling rate (V_r), structural features (N_A, f^{α} and f^{other}) and the alloy's composition. As expected, an increase in the ferrite fraction decreases LE, UTS and D, and increases slightly rupture elongation. The most noticeable effect is that of the cooling rate which dramatically affects tensile and yield strengths as well as hardness.

Acknowledgments

The authors would like to thank the financial support obtained from the Centro para el Desarrollo Tecnológico Industrial (CDTI) of the Spanish Government (ref. IDI 20071064).

References

[1] B.V. Kovacs: AFS Trans. Vol. 89 (1981), p. 79-96
[2] E.N. Pan, M.S. Lou and C.R. Loper: AFS Trans. Vol. 95 (1987), p. 819-840
[3] L. Guerin and M. Gagne: The Foundryman Vol. 80 (1987), p. 336-344
[4] G.M. Goodrich and R.W. Lobenhofer: AFS Trans., paper 07-045 (2007)
[5] J. Sertucha, P. Larrañaga, J. Lacaze and M. Insausti: Int. J. Metalcasting Vol. 4 (2010), p 51-58
[6] J. Sertucha, R. Suárez, J. Izaga, L.A. Hurtado and J. Legazpi: IJCMR Vol. 16 (2006), p. 315-322
[7] H. Takeda, K. Asano and H. Yoneda: Int. J. Cast Met. Res. Vol. 21 (2008), p. 81-85
[8] T. Levin, P.C. Rosenthal, C.R. Loper and R.W. Heine: AFS Trans Vol. 79 (1971) 493-514
[9] T. Kanno, T. Kikuchi, I. Kang and H. Nakae: AFS Trans., paper 05-203 (2005)
[10] G.S. Cho, K.H. Choe, K.W. Lee and A. Ikenaga: J. Mater. Sci. Tech. Vol. 23 (2007), p. 97-101
[11] G.H. Hsu, M.L. Chen and C.J. Hu: Mater. Sci. Eng. A, Vol. A444 (2007), p. 339-346
[12] I. Riposan, M. Chisamera and S. Stan: Int. J. Cast Met. Res. Vol. 20 (2007), p. 64-67
[13] T. Nobuki, M. Hatate and T. Shiota: Int. J. Cast Met. Res. Vol. 21 (2008), p. 31-38
[14] D.R. Askeland and S.S. Gupta: AFS Trans. Vol. 83 (1975), p. 313-320
[15] J. Lacaze J., C. Wilson C. and E. Dubu: Scand. J. Metallurgy Vol. 22 (1993), p. 300-309
[16] T. Watmough, W.F. Shaw and F.C. Bock: AFS Trans. Vol. 79 (1971), p. 225-246
[17] L.A. Neumeier, B.A. Betts and D.H. Desy: AFS Trans. Vol. 82 (1974), p. 131-138
[18] D. Venugopalan and A. Alagarsamy: AFS Trans. Vol. 98 (1990), p. 395-400
[19] A. Louvo, E. Pellikka, J. Alhainen and P. Eklund: AFS Trans. Vol. 99 (1991), p. 237-244
[20] X. Guo, D.M. Stefanescu, L. Chuzhoy, M.A. Pershing and G.L. Biltgen: AFS Trans. Vol. 105 (1997), p. 47-53
[21] L.E. Björkegren and K. Hamber, in: *Proceedings of the Keith Millis Symposium on Ductile Iron*, (2003)
[22] E.F. Ryntz: AFS Trans. Vol. 82 (1976), p. 551-554
[23] in: *Reference microstructure for measurement of pearlite and ferrite content in ductile iron microstructures*, AFS current information report, Quality Control Committee 12-E, Ductile Iron Division (1984)
[24] A.P. Druschitz, W.W. Chaput: AFS Trans. Vol. 101 (1993), p. 447-458
[25] S.K. Yu and C.R. Loper: AFS Trans. Vol. 96 (1988), p. 811-822
[26] D.E. Kippola and G.M. Goodrich: AFS Trans. Vol. 108 (2000), p. 313-320.